

Algorithm Theoretical Baseline Document

Meteosat Solar Surface Radiation and effective Cloud Albedo Climate Data Records - Heliosat

SARAH-2.1


The MAGIC SOL method applied for the generation of SARAH-2.1

[DOI: 10.5676/EUM_SAF_CM/SARAH/V002_01](https://doi.org/10.5676/EUM_SAF_CM/SARAH/V002_01)

Effective Cloud Albedo (CAL)	CM-23082 / CM-23085
Surface Incoming Shortwave Radiation (SIS):	CM-23202 / CM-23205
Surface Direct Irradiance (SDI):	CM-23291 / CM-23295
Spectrally Resolved Irradiance (SRI):	CM-23241 / CM-23245
Sunshine Duration (SDU):	CM-23282 / CM-23283

Reference Number:
Issue/Revision Index:
Date:

SAF/CM/DWD/ATBD/METEOSAT/HEL
2.4
22.01.2019

	Algorithm Theoretical Basis Document Meteosat Climate Data Records of Surface Radiation SARAH-2.1	Doc. No: SAF/CM/DWD/ATBD/METEOSAT/HEL Issue: 2.4 Date: 22.01.2019
---	--	--

Document Signature Table

	Name	Function	Signature	Date
Author	Jörg Trentmann Uwe Pfeifroth	CM SAF scientists		31.10.2018
Review	Rainer Hollmann	CM SAF Science Coordinator		31.10.2018 17.01.2019
Approval	CM SAF Steering Group			04.12.2018
Release	Martin Werscheck	Project Manager		22.01.2019


Distribution List

Internal Distribution	
Name	No. Copies
DWD Archive	1
CM SAF Team	1

External Distribution		
Company	Name	No. Copies
PUBLIC		1

Document Change Record

Issue/ Revision	Date	DCN No.	Changed Pages/Paragraphs
1.0	01/09/2013	SAF/CM/DWD/ATBD/METEOSAT/HEL	First official version.
1.1	02/12/2013	SAF/CM/DWD/ATBD/METEOSAT/HEL	Review Comments included
1.2	08/08/2014	SAF/CM/DWD/ATBD/METEOSAT/HEL	Added/modified paragraph 4.4 about the used aerosol information
1.3	01/11/2014	SAF/CM/DWD/ATBD/METEOSAT/HEL	Modifications according DRR2.1 review comments.
2.0	14/08/2015	SAF/CM/DWD/ATBD/METEOSAT/HEL	Update for MVIRI/SEVIRI Ed. 3
2.1	20/08/2016	SAF/CM/DWD/ATBD/METEOSAT/HEL	Update for DRR 2.8/2.9 and SARAH-2
2.2	29/11/2016	SAF/CM/DWD/ATBD/METEOSAT/HEL	Modifications according DRR2.8/2.9 review comments.
2.3	31/10/2018	SAF/CM/DWD/ATBD/METEOSAT/HEL	Update due to SARAH-2 extension until 2017
2.4	22/01/2019	SAF/CM/DWD/ATBD/METEOSAT/HEL	Final Editing and Layout modification to CDOP 3 Layout

	Algorithm Theoretical Basis Document Meteosat Climate Data Records of Surface Radiation SARAH-2.1	Doc. No: SAF/CM/DWD/ATBD/METEOSAT/HEL Issue: 2.4 Date: 22.01.2019
---	--	--

Applicable Documents

Reference	Title	Code
AD 1	CM SAF Product Requirements Document	SAF/CM/DWD/PRD/3.1
AD 2	Requirements Review Document	SAF/CM/CDOP2/DWD/RR28/1.1

Reference Documents

Reference	Title	Code
RD 1	Algorithm Theoretical Baseline Document, Meteosat (MVIRI) Solar Irradiance and effective Cloud Albedo Climate Data Sets, MVIRI_HEL; The MAGIC SOL method	SAF/CM/DWD/ATBD/MVIRI_HEL/1.2
RD 2	Algorithm Theoretical Baseline Document, Spectrally Resolved Solar Surface Irradiance, SRI	SAF/CM/DWD/ATBD/SRI/1.1

Table of Contents

1	The EUMETSAT SAF on Climate Monitoring (CM SAF).....	5
2	Introduction	7
3	The Heliosat method	9
3.1	The original Heliosat algorithm.....	9
3.2	From Heliosat to MAGIC SOL.....	9
3.3	Self calibration	9
3.4	Clear sky reflection	10
3.5	Correction for Viewing Geometry	10
3.6	Input data.....	11
3.7	Effective cloud albedo (CAL).....	12
3.8	Uncertainty of the effective cloud albedo retrieval	13
3.9	Limitations, assumptions and future improvements.....	14
3.10	Relation of the effective cloud albedo to solar irradiance	14
4	The gnu-MAGIC / SPECMAGIC algorithm.....	16
4.1	Solar irradiance: Introduction and Definition.....	16
4.2	Motivation and strategy for solar surface irradiance and direct irradiance	16
4.3	Algorithm Overview.....	16
4.4	Atmospheric input information.....	17
5	Solar surface radiation (SIS / DNI / SRI).....	19
5.1	Averaging	19
5.2	Sensitivity and dependence on input parameters of SIS / SDI / SRI.....	20
5.3	Assumption, limitations and future improvements	21
6	Sunshine Duration.....	23
6.1	Weighting of sunny slots	23
6.2	Assumption, limitations and future improvements	24
7	Improvements relative to the released previous versions of the CM SAF Surface Radiation data records.	25
7.1	Improvements compared to the MVIRI Surface Radiation data record.....	25

7.2 Improvements compared to the first version of SARAH data record (MVIRI/SEVIRI Ed.2) 25

8 References.....27

9 Glossary – List of Acronyms30

List of Figures


Figure 3-1: Normalized spectral responses for the broadband visible channel of MVIRI and the two visible bands of SEVIRI. Also shown is the normalized solar spectral irradiance (Figure taken from Cros et al., 2006). 11

Figure 4-1: The relation of the transmission to a manifold of atmospheric states is pre-calculated with a radiative transfer model (RTM) and saved in a look-up table (LUT). Once, the LUT has been computed the transmittance for a given atmospheric state can be extracted from the LUT for each satellite pixel and time. 17

Figure 5-1: Diagram of the interface of gnu-MAGIC / SPECMAGIC to the atmospheric input and the satellite observations, CeFF stands for the dark offset corrected and normalised Counts. 19

List of Tables

Table 2-1: Overview of Meteosat based data records discussed in this ATBD. 8

	Algorithm Theoretical Basis Document Meteosat Climate Data Records of Surface Radiation SARAH-2.1	Doc. No: SAF/CM/DWD/ATBD/METEOSAT/HEL Issue: 2.4 Date: 22.01.2019
---	--	--

1 The EUMETSAT SAF on Climate Monitoring (CM SAF)

The importance of climate monitoring with satellites was recognized in 2000 by EUMETSAT Member States when they amended the EUMETSAT Convention to affirm that the EUMETSAT mandate is also to “contribute to the operational monitoring of the climate and the detection of global climatic changes”. Following this, EUMETSAT established within its Satellite Application Facility (SAF) network a dedicated centre, the SAF on Climate Monitoring (CM SAF, <http://www.cmsaf.eu>).


The consortium of CM SAF currently comprises the Deutscher Wetterdienst (DWD) as host institute, and the partners from the Royal Meteorological Institute of Belgium (RMIB), the Finnish Meteorological Institute (FMI), the Royal Meteorological Institute of the Netherlands (KNMI), the Swedish Meteorological and Hydrological Institute (SMHI), the Meteorological Service of Switzerland (MeteoSwiss), the Meteorological Service of the United Kingdom (UK MetOffice) and the Centre National de la recherche scientifique (CNRS) of France. Since the beginning in 1999, the EUMETSAT Satellite Application Facility on Climate Monitoring (CM SAF) has developed and will continue to develop capabilities for a sustained generation and provision of Climate Data Records (CDR’s) derived from operational meteorological satellites.

In particular the generation of long-term data records is pursued. The ultimate aim is to make the resulting data records suitable for the analysis of climate variability and potentially the detection of climate trends. CM SAF works in close collaboration with the EUMETSAT Central Facility and liaises with other satellite operators to advance the availability, quality and usability of Fundamental Climate Data Records (FCDRs) as defined by the Global Climate Observing System (GCOS). As a major task the CM SAF utilizes FCDRs to produce records of Essential Climate Variables (ECVs) as defined by GCOS. Thematically, the focus of CM SAF is on ECVs associated with the global energy and water cycle.


Another essential task of CM SAF is to produce data records that can serve applications related to the new Global Framework of Climate Services initiated by the WMO World Climate Conference-3 in 2009. CM SAF is supporting climate services at national meteorological and hydrological services (NMHSs) with long-term data records but also with data records produced close to real time that can be used to prepare monthly/annual updates of the state of the climate. Both types of products together allow for a consistent description of mean values, anomalies, variability and potential trends for the chosen ECVs. CM SAF ECV data records also serve the improvement of climate models both at global and regional scale.

As an essential partner in the related international frameworks the CM SAF assumes the role as main implementer of EUMETSAT’s commitments in support to global climate monitoring. This is achieved through:

- Application of highest standards and guidelines as lined out by GCOS for the satellite data processing,
- Processing of satellite data within an international collaboration benefiting from developments at international level and pollinating the partnership with own ideas and standards,
- Intensive validation and improvement of the CM SAF climate data records,
- Taking a major role in data record assessments performed by research organisations such as WCRP (World Climate Research Programme),
- Maintaining and providing an operational and sustained infrastructure that can serve the community within the transition of mature CDR products from the research community into operational environments.

	Algorithm Theoretical Basis Document Meteosat Climate Data Records of Surface Radiation SARAH-2.1	Doc. No: SAF/CM/DWD/ATBD/METEOSAT/HEL Issue: 2.4 Date: 22.01.2019
---	--	--

A catalogue of all available CM SAF products is accessible via the CM SAF webpage, www.cmsaf.eu. Here, detailed information about product ordering, add-on tools, sample programs and documentation is provided.

	Algorithm Theoretical Basis Document Meteosat Climate Data Records of Surface Radiation SARAH-2.1	Doc. No: SAF/CM/DWD/ATBD/METEOSAT/HEL Issue: 2.4 Date: 22.01.2019
---	--	--

2 Introduction

The generated 35 year long (1983-2017) continuous surface radiation climate data records are based on observations from the Meteosat First and Second Generation satellites; it is the second release of the SARAH data record (SARAH-2) together with the extension for the years 2016 and 2017. The Digital Object Identifier (DOI) of this SARAH-2.1 data record (1983-2017) is 10.5676/EUM_SAF_CM/SARAH/V002_01 and includes the SARAH-2 data record (1983-2015) (DOI: 10.5676/EUM_SAF_CM/SARAH/V002).

For climate monitoring and climate analysis time series of climate variables of sufficient length (i.e., spanning multiple decades) are required. To generate such long time series, the satellite information of the first generation of Meteosat satellites (Meteosat-2 to Meteosat-7, covering 1982 to 2005) has to be employed. The MVIRI instrument on-board the Meteosat First Generation satellite is equipped with 3 channels: a broadband channel in the visible, a channel in the infrared, and a water vapor channel.

The second generation of Meteosat satellites (Meteosat-8 to (currently) Meteosat-10, covering 2005 to today) is equipped with the Spinning Enhanced Visible and Infrared Imager (SEVIRI) and the Geostationary Earth Radiation Budget (GERB) instrument. The GERB instrument is a visible-infrared radiometer for earth radiation budget studies. It provides accurate measurements of the shortwave (SW) and longwave (LW) components of the radiation at the top of the atmosphere. SEVIRI employs twelve spectral channels, which provide more information of the atmosphere compared to its forerunner. Several retrieval algorithms have been developed to use the additional information gained by the improved spectral information of MSG mainly for nowcasting applications. However, these algorithms can not be applied to the MVIRI instrument on-board the Meteosat First Generation satellites as they use spectral information that is not provided by MFG (e.g., the NWC SAF cloud algorithm, the CM SAF operational radiation algorithm).

As a consequence, in order to be able to provide a long time series covering more than 20 years, a specific climate algorithm has to be applied to the satellite observations from the First and Second Generation of Meteosat satellites.

The MAGIC SOL method is a combination of the well established Heliosat method (see Section 3) with the SPEC MAGIC clear-sky model, based on the gnu-MAGIC clear sky model. MAGIC SOL does meet the above mentioned requirements. The method provides the effective cloud albedo, the solar surface irradiance, and the net shortwave radiation, i.e., relevant components of the GCOS Essential Climate Variables (ECVs) surface radiation budget and cloud properties.

The MAGIC SOL method requires as satellite information only the measurements of the broadband visible channel and can therefore be applied across different satellite generations. The application to observations from other geostationary satellites, e.g., GOES and GMS, is also possible. Hence, the MAGIC SOL method has not only the power to provide long time series of ECVs, but also to provide ECVs, which cover the complete geostationary ring.

The basis of the cloud part of the MAGIC SOL method is the Heliosat method, which is well established in the solar energy community. However, modifications of the original Heliosat method were needed to meet the requirements to generate a Climate Data Record. This modification is discussed in Section 3.3.

In comparison to the method and input data used for the generation of the first MVIRI-only climate data record of the CM SAF (RD.1) the following modifications have been performed.

The method for the retrieval of the clear sky reflection has been modified. The method applied for the generation of the current data record is discussed in Section 3.4. The modification was needed because the former approach (Fuzzy logic approach, see RD.1) led

to artefacts in the effective cloud albedo. Additionally a bug in the routine for the calculation of the scanning time of the pixels has been fixed. An updated aerosol climatology has been used. This climatology accounts for the detection of thick aerosol plumes in the Heliosat method and reduces the uncertainty of the data record (Mueller et al. 2015a). The image data of Meteosat First generation has been visually inspected (1983-1994). Corrupt images have been either corrected or have been not used for the processing of the climate data record.


In addition to the extra parameters in the second release of the SARAH data record, SRI and SDU, also the retrieval algorithm has been slightly modified. In particular a correction of the cloud albedo has been implemented to account for slant viewing geometry effects. This results in an improved performance of the retrieval, especially in higher latitudes. Monthly mean total ozone data from ERA-Interim is used for the calculation of the clear-sky radiation. The integrated water vapour has been adjusted to account for topographic effects.

All modifications relative to RD.1 and to the first version of the SARAH data record are summarized in Section 6.

The generated long-term continuous surface radiation climate data record is based on observations from the Meteosat First and Second Generation satellites and is called SARAH: Surface Solar Radiation Data record – Heliosat. This document reports the algorithm used to derive the second version of the SARAH data record. An overview of the SARAH-2 climate data record and the algorithm used for its generation is also given by Mueller et al., 2015b.

Table 2-1: Overview of Meteosat based data records discussed in this ATBD.

Acronym	Product title	Unit
SIS	Surface Incoming Shortwave Irradiance	W/m ²
CAL	Effective Cloud Albedo	Dimensionless
SDI	Surface Direct Irradiance	W/m ²
SRI	Spectral Resolved Irradiance	W/m ²
SDU	Sunshine Duration	h

	Algorithm Theoretical Basis Document Meteosat Climate Data Records of Surface Radiation SARAH-2.1	Doc. No: SAF/CM/DWD/ATBD/METEOSAT/HEL Issue: 2.4 Date: 22.01.2019
---	--	--

3 The Heliosat method

3.1 The original Heliosat algorithm

The Heliosat algorithm uses reflection measurements given as normalized digital counts to determine the effective cloud albedo, also called cloud index (Beyer et al. 1996; Cano et al. 1986; Hammer et al. 2003). A clear sky model is used afterwards to calculate the solar surface irradiance based on the retrieved effective cloud albedo. Basis of the Heliosat method are the digital counts of the visible Meteosat channel. No information from NIR or IR channels is required.

The first step in the Heliosat method is the retrieval of the effective cloud albedo (cloud index), n , i.e. the normalised relation between the all sky and the clear sky reflection in the visible channel observed by the satellite:

Equation 3-1

$$n = \frac{\rho - \rho_{srf}}{\rho_{max} - \rho_{srf}}$$

Here, ρ is the observed reflection for each pixel and time in counts. ρ_{sfc} is the clear sky reflection, and ρ_{max} is an estimate for the maximum reflectivity observed by the satellite. Further details on the calculation of the effective cloud albedo can be found in RD 1, Section 3.1.

3.2 From Heliosat to MAGIC SOL

To meet the requirements of a CDR some modifications of the original Heliosat algorithm have been performed, resulting in a version of the Heliosat algorithm for the generation of climate data records. In particular a self-calibration algorithm (see Section 3.3), which dynamically accounts for changes in sensor sensitivity, has been developed. The modified version of the Heliosat algorithm in combination with the gnu-MAGIC / SPECMAGIC approach (see Section 4) is called MAGIC SOL.

The MAGIC SOL approach has been used in the processing of the CM SAF Surface Radiation data record based on the MVIRI instruments on-board the first generation of Meteosat satellites (Posselt et al., 2012). Full details of the algorithm are presented in RD 1, Posselt et al. (2012) and Müller et al. (2015). Here an overview of the method is provided.

3.3 Self calibration

The self-calibration algorithm is based on an operational and automatic determination of the maximum reflectivity ρ_{max} . In analogy to (Rigollier et al. 2002) a histogram of all available counts is generated and the 95th-percentile is used as self-calibration parameter and set to ρ_{max} (Hammer et al., 2003 and references therein). Only satellite pixels located in the southern Atlantic between 15° W and 0° W and 58° S and 48° S are considered. This region features a high abundance of frontal systems with large cloud amounts most of the time, but hardly any convection. The statistical analysis is based on one month of satellite data at 13 UTC. The resulting estimate for ρ_{max} is then applied to all slots within that month.

Further details and a validation of the self calibration method can be found in Posselt et al. (2012) and RD 1.

3.4 Clear sky reflection

The processing of the long time series of surface solar radiation from the geostationary Meteosat satellites employs a robust clear sky or background reflection method based on Hammer (2000). This method replaces the method of (Dürr and Zelenka 2009), which was used in the processing of the CM SAF MVIRI-based surface radiation data record (Posselt et al., 2012). While the previously used method works well over snow covered regions, it has some weakness over desert regions.

The clear sky reflection is derived from the frequency distribution of the observed reflections during an appropriate time period. This frequency distribution exhibits one peak for cloudy and a separate peak for clear sky reflection. The peak for clear sky reflection is usually significantly lower and at the lower end of the overall frequency distribution, the dark counts. Hence, the clear sky reflection can be estimated by a minima approach. Using the lowest value of the reflection within a certain time period might be an option. However, the lowest values are often a result of cloud shadows and therefore do not represent the clear sky reflection. Hence, the clear sky reflection can be interpreted as a stationary variate with a mean value ρ_{sfc} and a variance ε . All values above a starting value ρ_{sfc} plus the ε are iteratively sorted out. After each iteration step a new mean is derived, hence a new limit for the sorting applies.

The iteration process is given in Equation 3-2, the calculated mean iterates to the clear sky reflection ρ_{sfc} if Equation 3-3 is fulfilled. Here ρ_{cld} and ε_{cld} are the respective values for clouds:

Equation 3-2

$$\begin{aligned} \text{starting value : } & \rho_{srf} = \max(\text{datarange}) \\ \text{iteration : if } & (\rho < \rho_{srf} + \varepsilon) \rightarrow \rho_{srf} = \rho \\ & (\text{change}) \\ \text{else : } & \rightarrow \rho_{srf} = \rho_{srf} \\ & (\text{no change}) \end{aligned}$$

Equation 3-3

$$\rho_{cld} - \rho_{srf} > \max(\varepsilon, \varepsilon_{cld})$$

The clear sky reflection is derived for every pixel and every slot. The time series has to be long enough to contain cloudless conditions for every pixel. However, the time series should be also short enough to consider seasonal changes in the surface albedo. Hence, a time span of about 1 month is assumed to be appropriate and widely used. The surface albedo exhibits a strong dependency on the solar zenith angle. The surface albedo in turn is the driving factor for the clear sky reflection. Hence, the method is applied for every slot, in order to resolve the solar zenith angle dependency. As the mean of the dark counts is used values of CAL smaller than 0 might occur.

3.5 Correction for Viewing Geometry

Due to the longer atmospheric path the detection of clouds is artificially enhanced at larger satellite zenith angles resulting in an underestimation of surface solar radiation in the outer regions of the Meteosat disc. This effect is empirically parameterized as a function of the satellite zenith angle, Θ_{sat} :

Equation 3-4

$$Corr = 0.1 * (\cos\left(\frac{\theta_{sat}}{1.13}\right)^{1.3})^{-0.9} - 1$$

To apply the correction factor only under moderate CAL conditions, the correction is applied for $CAL > 0.04$ and $CAL * \theta_{sat} / 1.3 < 0.55$:

Equation 3-5

$$n = n * (1 - Corr)$$

3.6 Input data

From the MVIRI instruments on-board the first generation of Meteorol satellites the rectified digital pixel counts of the broadband visible MVIRI channel are used. The respective data are called “*Rectified Image Data*” and provided by EUMETSAT (EUM TD 06) in openMTP format. However, other formats and satellite images can be treated as well. Rectified images containing counts are used.

The SEVIRI instruments on-board the Second Generation of Meteorol Satellites do not continue to provide the same spectral broadband information as the MVIRI instruments. For a consistent prolongation of the time series from the MVIRI instruments broadband observations have to be used (Posselt et al., 2011). A linear combination of the MSG/SEVIRI visible narrowband channels (VIS006 and VIS008) will be used (Cros et al., 2006, see **Figure 3-1**). This approach has been proven to enable a homogeneous retrieval of surface solar radiation between MFG and MSG (Posselt et al., 2013).

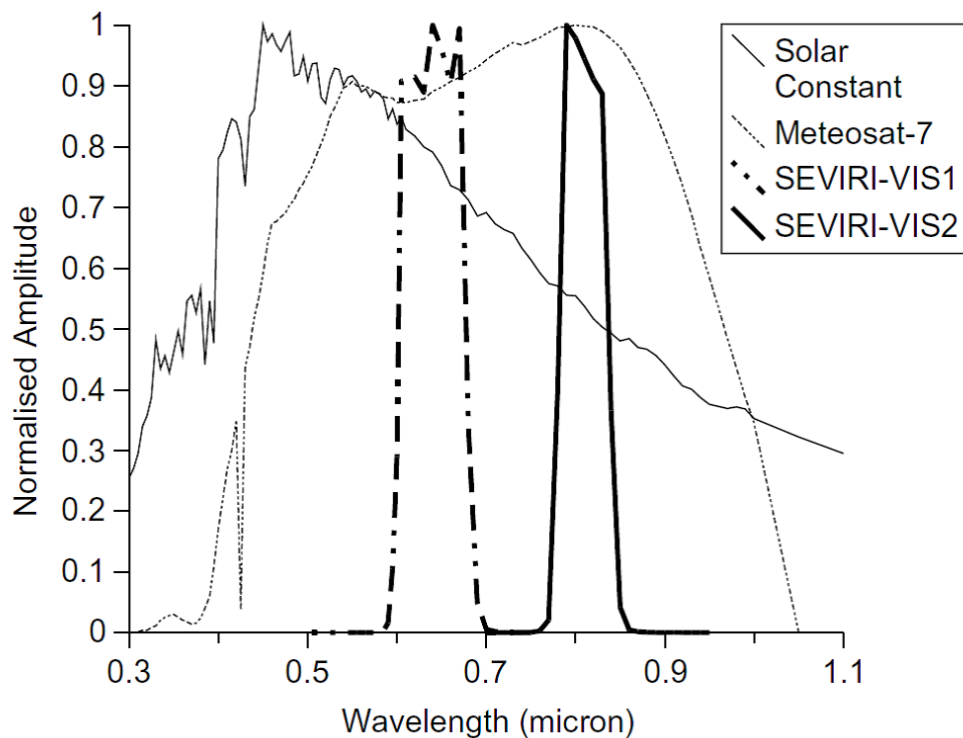



Figure 3-1: Normalized spectral responses for the broadband visible channel of MVIRI and the two visible bands of SEVIRI. Also shown is the normalized solar spectral irradiance (Figure taken from Cros et al., 2006).

	Algorithm Theoretical Basis Document Meteosat Climate Data Records of Surface Radiation SARAH-2.1	Doc. No: SAF/CM/DWD/ATBD/METEOSAT/HEL Issue: 2.4 Date: 22.01.2019
---	--	--

The first MVIRI climate data record of CM SAF shows stripe artefacts in the radiation products, due to similar features in the MVIRI raw images. Therefore all MVIRI raw images covering the time period 1983-1994 have been visually inspected. It has been found that a lot of raw images of Meteosat First Generation show so far undocumented stripes. For those images only every second line is defined, resulting in stripes in the surface radiation products as well. For SARAH the missing scan lines have been filled by spatial-temporal interpolation in order to have sufficient images for the processing and to gain the optimal information content out of the images. Images with unfixable bugs have been identified and have been not used for the processing.

3.7 Effective cloud albedo (CAL)

The effective cloud albedo is derived with the MAGIC SOL method described the previous sections. Clouds have a net cooling effect, which is several magnitudes higher than the forcing caused by the increase of greenhouse gases. Every trend and anomalies in the effective cloud albedo would significantly affect the climate system on a global and/or regional scale. However, despite its relevance for the climate system, it has not yet been classified as an essential climate variable by GCOS. As clouds can be assumed as Lambertian surfaces, the derived quantity can be considered the effective cloud albedo.

It is important to note that the effective cloud albedo does depend on the cloud reflectivity and the surface albedo. The same cloud has a larger effective cloud albedo over a dark surface (e.g., ocean) than over a bright surface (e.g., desert). For the assessment of the radiative impact of clouds on the reflected solar radiation the effective cloud albedo is the relevant cloud radiative property.

3.7.1 Averaging


Monthly and daily means of the effective cloud albedo are calculated by arithmetic averaging, using Equation 3-6:

Equation 3-6

$$CAL_{mean} = \frac{\sum_{i=1}^n CAL_i}{n}$$

Here n corresponds to the number of available instantaneous cloud albedo data per day for the calculation of the daily mean or to the number of available daily means for the calculation of the monthly means. A minimum number of 5 available instantaneous cloud albedo data sets per day is required to derive the daily mean for this specific pixel. The required minimum number of CAL measurements for the calculation of the daily means is a compromise between accuracy requirements and resulting data availability. No daily mean CAL data is provided in case the daily mean of SIS is not available. The monthly average is calculated from the daily means of this month for each pixel as the arithmetic mean with a required number of 10 existing daily means.

The conversion from the irregular satellite projection to the regular 0.05 x 0.05 degree regular lon-lat-grid is conducted with the gnuMAGIC gridding tool based on a nearest-neighbour method.

	Algorithm Theoretical Basis Document Meteosat Climate Data Records of Surface Radiation SARAH-2.1	Doc. No: SAF/CM/DWD/ATBD/METEOSAT/HEL Issue: 2.4 Date: 22.01.2019
---	--	--

3.8 Uncertainty of the effective cloud albedo retrieval

The uncertainty associated with the retrieval of the effective cloud albedo can be estimated based on the sensitivity of CAL on the parameters used in the retrieval of CAL. Here the main results of the sensitivity assessment are summarized, details can be found in RD 1.

3.8.1 Sensitivity of the effective cloud albedo on ρ_{\max} and ρ_{srf}

The effective cloud albedo is defined as a relative quantity of observed satellite counts.. Hence, any noise or uncertainty in the absolute calibration of the satellite observations cancels out. The uncertainty in the effective cloud albedo is therefore pre-dominantly determined by uncertainties in the determination of the clear sky reflection and the self-calibration method.

3.8.2 Sensitivity of CAL on self-calibration method

The uncertainty or fuzziness in ρ_{\max} defined by the month to month variations of ρ_{\max} is in the order of 3%. However, it is likely that part of this uncertainty is due to the variability in the satellite counts, which will cancel out in the calculation of the effective cloud albedo (Equation 3-1), and, hence, do not affect the accuracy of CAL. Under the worst case assumption of an uncertainty of ρ_{\max} of 3% the uncertainty of CAL is in the order of 5 % over bright surfaces. However, such high uncertainties occur only for high CAL values, hence the effect on solar irradiance is rather low. Further information can be found in RD 1.

3.8.3 Sensitivity of CAL on clear sky reflection

The impact of the uncertainty in the determination of the clear sky reflection on the effective cloud albedo is low as a consequence of the occurrence of ρ_{srf} in the dominator and nominator of the effective cloud albedo formula.

However, the clear sky reflection can introduce significant uncertainty in the effective cloud albedo retrieval for the case of cloud contamination. This happens if not enough clear sky cases occur. Hence, for regions with long-lasting cloud cover in combination with slant geometry the ρ_{srf} retrieval fails to see the clear sky situations, hence ρ_{srf} is contaminated by clouds and not representative for clear sky conditions. This effect occurs pre-dominantly at the border of the Meteosat disk, above 60 degrees viewing angle. As it occurs only for regions with long-lasting cloud coverage (hence large values of the effective cloud albedo) the effect on the solar irradiance is much lower as implied by the uncertainty in the effective cloud albedo. Further information and graphical illustrations of these effects can be found in RD 1.

3.9 Limitations, assumptions and future improvements

Below is a list of some known deficiencies and limitations of the algorithm to derive CAL:

- The clear sky reflection, ρ_{sfc} , can accurately be retrieved if a certain number of clear sky cases are available within a month. This is not always the case.
- Snow-covered surfaces might be interpreted as clouds by the algorithms, resulting in an overestimation of the effective cloud albedo.
- Neglecting the anisotropic reflection of clouds introduces some uncertainty to the derived effective cloud albedo. While this assumption is thought to be a good approximation for low level water clouds, the scattering function of high level ice clouds might not follow this assumption.

3.10 Relation of the effective cloud albedo to solar irradiance

The ratio of the all-sky surface solar radiation and the clear-sky surface solar radiation is the clear sky index:

Equation 3-7
$$k = SIS / SIS_{CLS}$$

Hence, the all-sky surface solar radiation can be derived as the product of the clear-sky index and the clear-sky surface solar radiation:

Equation 3-8
$$SIS = k \cdot SIS_{CLS}$$

Here SIS_{CLS} is the solar irradiance for cloud free skies. For most conditions, the effective cloud albedo, CAL, can be related to the clear sky index by:

Equation 3-9
$$k = 1 - CAL$$

This relation is defined by the law of energy conservation (Dagestad, 2004). For CAL values below -0.2 and above 0.8 empirical corrections are required:

Equation 3-10

CAL < -0.2:	$k=1.2$
-0.2 < CAL < 0.8	$k = 1 - CAL$
0.8 < CAL < 1	$k = 2.0667 - 3.6667 \cdot CAL + 1.6667 \cdot CAL^2$
CAL > 1.1	$k = 0.05$

Based on the diffuse model of Skartveit et al. (1998) the direct solar radiation, SID, is derived from the clear-sky index using the following formula

Equation 3-11
$$SID_{allsky} = SID_{CLS} (k - 0.38 \cdot (1 - k))^{2.5}$$

For values of the cloud albedo larger than 0.6 the direct irradiance is zero, which is in line with observations (Skartveit et al., 1998). The direct normalized irradiance, DNI, is derived from SID by normalisation with the cosine of the solar zenith angle (SZA):

Equation 3-12
$$DNI = SID / \cos(SZA)$$

To account for the spectral dependency of the cloud effect described by the clear-sky index, the broadband spectral index, k , needs to be adjusted to result in a spectral dependent clear sky index, k^{wb} , for each of the considered 32 wavelength bands. These conversion factors, f^{wb} , have been determined for different values of the cloud albedo using radiative transfer calculations with the RTM libradtran and are shown in Figure 3-1. The spectrally-resolved clear sky index, k^{wb} , can then be derived from the broadband clear sky index:

Equation 3-13 $k^{wb} = f^{wb} * k$

The spectrally resolved irradiance is finally derived by application of Equation 3-14:

Equation 3-14 $SIS^{wb} = k^{wb} * SIS^{wb}_{cls}$

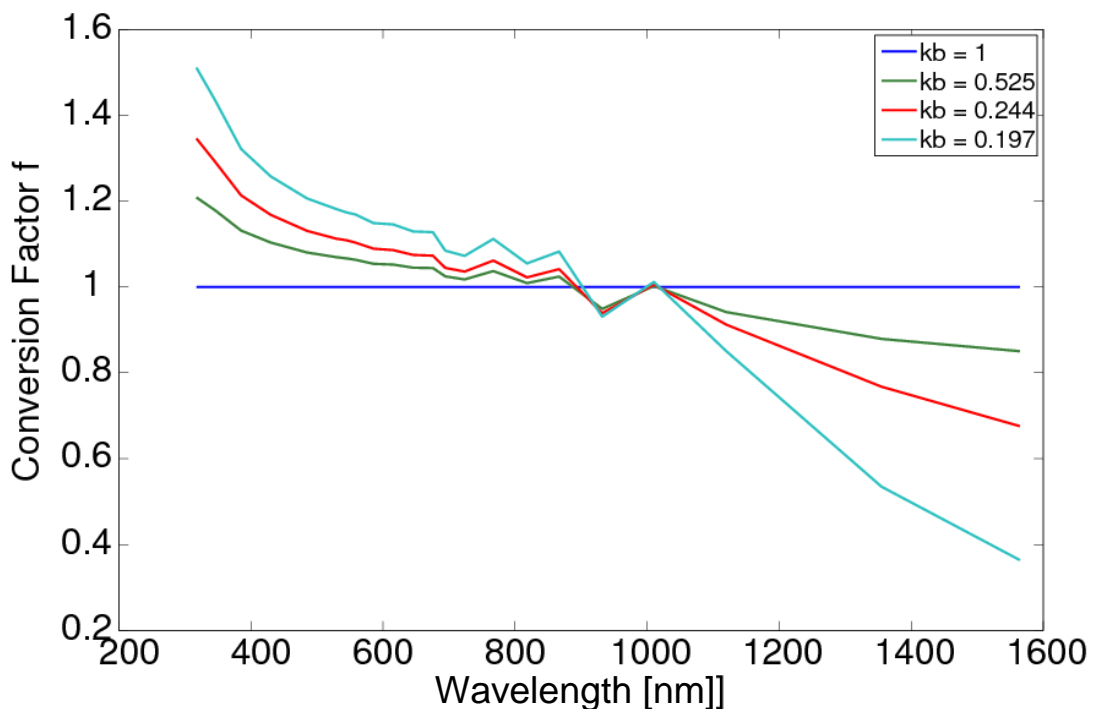



Figure 3-1: The conversion factors, f^{wb} , for the spectral resolved effective cloud albedo as a function of broadband clear sky index, kb .

More details on the calculation of the spectrally-dependent clear sky index can be found in RD 2 and Mueller et al. (2012).

With the knowledge of the wavelength-dependent clear sky index and the clear sky surface radiation components (global and direct), the all sky surface solar radiation can be derived using the equations given above. The clear sky solar irradiance is calculated using an eigenvector look-up table method (see Mueller et al. 2012; Mueller et al. 2009). It is based on radiative transfer modelling and enables the use of extended information about the atmospheric state. Further details of the clear sky atmospheric radiative transfer model are presented in Section 4.

	Algorithm Theoretical Basis Document Meteosat Climate Data Records of Surface Radiation SARAH-2.1	Doc. No: SAF/CM/DWD/ATBD/METEOSAT/HEL Issue: 2.4 Date: 22.01.2019
---	--	--

4 The gnu-MAGIC / SPECMAGIC algorithm

The clear sky solar irradiance is calculated using an eigenvector look-up table method (see Mueller et al. 2012; Mueller et al. 2009). It is based on radiative transfer modelling and enables the use of extended information about the atmospheric state. Accurate analysis of the interaction between the atmosphere, clear sky reflection, transmission and the top of atmosphere albedo has been the basis for this method, characterized by a combination of parameterizations and “eigenvector” look-up tables. A detailed description of the gnu-MAGIC algorithms can be found in RD 1 and Mueller et al. (2009); the extension of gnu-MAGIC, SPECMAGIC, to consider the spectral information and to derive the spectral resolved surface irradiance is described in RD 2 and Mueller et al. (2012).

4.1 Solar irradiance: Introduction and Definition

The solar surface irradiance consists of a diffuse fraction and a direct fraction. The diffuse fraction of the surface irradiance is defined as the solar radiation that has undergone scattering in the atmosphere. The direct irradiance is the flux reaching a horizontal unit of the earth’s surface in the 0.2 - 4 μm wavelength band from the direction of the sun without being scattered. Both quantities are expressed in W/m^2 .

4.2 Motivation and strategy for solar surface irradiance and direct irradiance

Accurate information on the direct and total solar irradiance is important for

- the monitoring, the analysis and the understanding of the climate system,
- the prediction of energy yield, the planning, monitoring and system design of photovoltaic systems and solar-thermal power plants
- agrometeorological applications.

Only few well-maintained ground measurements of irradiance (in particular, direct irradiance) exist in Europe, while in Africa and over the ocean almost no information on surface radiation is available from surface observations. Geostationary satellites enable the retrieval of area-wide total and direct irradiance in high spatial and temporal resolution with good accuracy ($<15 \text{ W}/\text{m}^2$).

In the previous years, CM SAF has already successfully extended and applied well-established methods used within the Solar Energy community (e.g., Skartveit et al., 1998) to generate surface solar radiation data records from satellite observations. One important extension of the clear sky surface radiation algorithm (gnu-MAGIC) is the use of detailed aerosol information instead of turbidity maps. The clear sky irradiance is completely based on Radiative Transfer Modelling. Finally, the possibility to use an improved cloud mask is expected to improve the accuracy. The physical basis of the algorithm is described in Mueller et al. (2009) and Müller et al. (2003).

4.3 Algorithm Overview

In the following the gnu-MAGIC / SPECMAGIC algorithm to derive the direct and the spectrally-resolved total surface radiation under clear sky conditions is briefly presented. A full description can be found in RD 1, RD 2, Mueller et al. (2009), and Mueller et al. (2012). The calculation of the surface clear sky direct irradiance and the surface clear sky solar surface irradiance is realised using an eigenvector look-up table (LUT) approach. The LUTs

for the surface direct and total solar radiation have been generated by conducting radiative transfer model (RTM) simulations using libRadtran (Mayer and Kylling, 2005) (Figure 4-1). A LUT is a data structure used to replace the time-consuming RTM computation with a simpler and faster interpolation operation within discrete pre-computed RTM results.

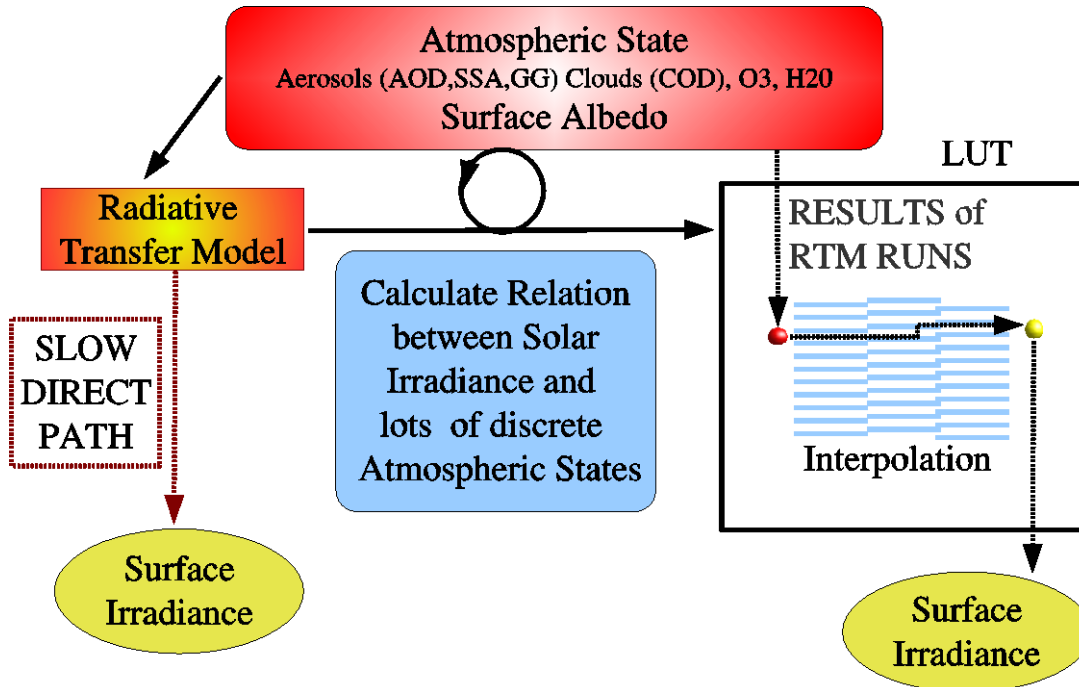



Figure 4-1: The relation of the transmission to a manifold of atmospheric states is pre-calculated with a radiative transfer model (RTM) and saved in a look-up table (LUT). Once, the LUT has been computed the transmittance for a given atmospheric state can be extracted from the LUT for each satellite pixel and time.

The clear sky LUTs consists of radiative transfer model results for aerosols with different aerosol optical thickness, single scattering albedo, and asymmetry parameter. Fixed values for water vapour, ozone and surface albedo have been used for the calculation of the basis LUT. The effect of the solar zenith angle on the transmission, hence the surface solar irradiance, is considered by the use of the Modified Lambert Beer (MLB) function (Mueller et al., 2004). The effects of water vapour and surface albedo on the surface radiation are considered using correction formulas and parameterizations. Therefore the MAGIC code is fast, robust and suitable for operational application.

The input parameters of the gnu-MAGIC / SPECMAGIC code are date, time, solar zenith angle, latitude, longitude, effective cloud albedo (cloud index), water vapour column density, surface albedo, aerosol optical thickness and single scatter albedo for aerosols. The output of the gnu-MAGIC 7 SPECMAGIC code is the spectrally-resolved (32 bands), the total and the direct clear sky surface solar irradiance in the 0.2-4.0 μm wavelength region. The extra terrestrial total solar irradiance is set to 1361 W/m^2 and adjusted according to the earth-sun distance. More details on the gnu-MAGIC / SPECMAGIC algorithm are described by Mueller et al. (2004, 2009, 2012).

4.4 Atmospheric input information

Here the atmospheric input information used to retrieve the clear sky surface solar irradiance is described.

	Algorithm Theoretical Basis Document Meteosat Climate Data Records of Surface Radiation SARAH-2.1	Doc. No: SAF/CM/DWD/ATBD/METEOSAT/HEL Issue: 2.4 Date: 22.01.2019
---	--	--

Aerosol:

Aerosol particles have a significant effect on the surface solar irradiance, because they scatter and absorb solar radiation. To describe the effect of scattering and absorption, information about the aerosol type and aerosol optical depth is needed. The aerosol type determines the relation between scattering and absorption, which is expressed by the single scattering albedo. The asymmetry parameter depends also on the aerosol type (size and composition) and determines the relation between forward- and backward-scattering. For the calculation of direct irradiance only the aerosol optical depth is relevant, as the AOD is defined as the attenuation of direct irradiance. The single scattering albedo and the asymmetry factor (both are determined by the aerosol type) are only of relevance for the total solar irradiance (diffuse + direct irradiance).

Monthly mean aerosol information is taken from an aerosol climatology by the European Centre for Medium Range Weather Forecast – MACC (Monitoring Atmospheric Composition and Climate). The MACC data results from a data assimilation system for global reactive gases, aerosols and greenhouse gases. It consists of a forward model for aerosol composition and dynamics (Morcrette et al., 2009) and the data assimilation procedure described in detail in (Benedetti et al., 2009). It has recently been used for the estimation of aerosol radiative forcing (Bellouin et al., 2013). The MACC reanalysis data is generated on a Gaussian T159 grid which corresponds to ~120 km resolution. For the use within CM SAF it has been regridded to a 0.5x0.5 degree regular latitude longitude grid.

The MACC aerosol information has been evaluated to perform significantly better than Kinne et al. and GADS/OPAC climatology (Hess et al., 1998, Köpke et al. 1997), see Mueller and Träger-Chatterjee (2014) for further details. The original MACC climatology has been adjusted to account for the detection of high aerosol loadings in the cloud index retrieval based on the study of Mueller et al. (2015a).

Water vapour:

Water vapour is an important atmospheric absorber in the solar spectral range. Monthly values of the vertically-integrated water vapour are taken from the ERA-Interim global reanalysis data record of ECMWF (Dee et al., 2011). A topographic correction is applied when regridding the integrated water vapour from ERA-Interim to 0.15 deg assuming a scale height of 1600 m based on Bento (2016).

Ozone:

Ozone is a strong absorber in the UV spectral range, but the absorption is quite weak within the broadband spectrum, which is relevant for the estimation of the direct irradiance. Here monthly mean values of the total integrated ozone column from ERA-Interim (Dee et al., 2011) are used.

All these external input parameters to the clear sky surface radiation algorithms are temporally and spatially interpolated to the satellite observations and used in the gnu-MAGIC / SPECMAGIC algorithm to derive the clear sky direct, the spectrally-resolved and the total surface radiation for every satellite measurement and each satellite pixel.

5 Solar surface radiation (SIS / DNI / SRI)

To derive the surface solar radiation under all-sky conditions, the clear sky information as derived from the SPECMAGIC algorithm (see Section 4) is combined with the information from the effective cloud albedo (see Section 3) using the formulas presented in Section 3.7. Figure 5-1 presents a schematic overview of the retrieval concept and the algorithm.

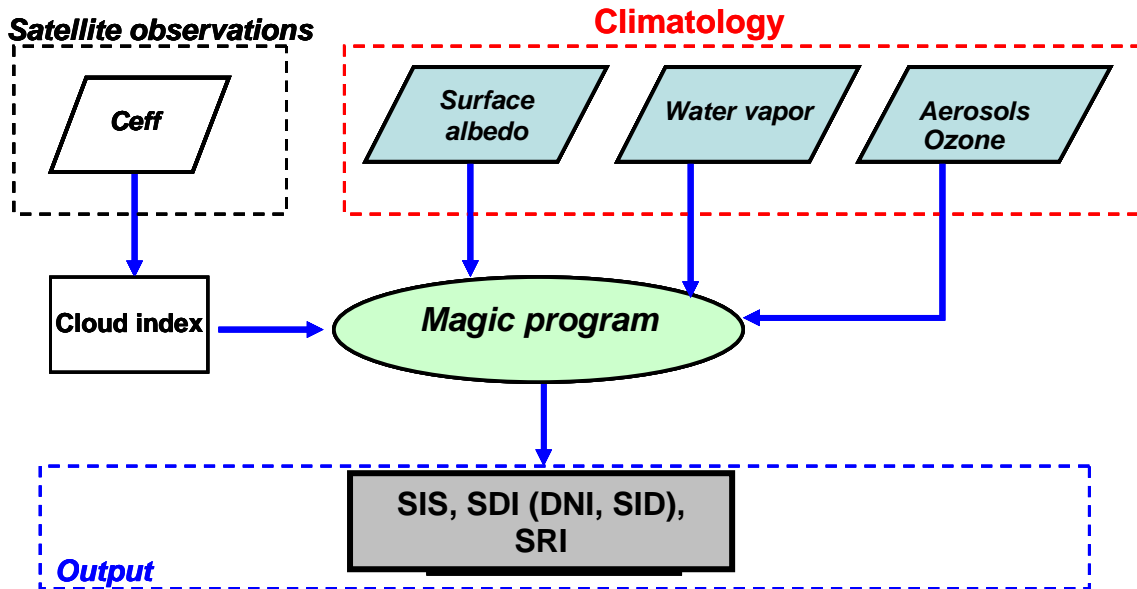


Figure 5-1: Diagram of the interface of gnu-MAGIC / SPECMAGIC to the atmospheric input and the satellite observations, Ceff stands for the dark offset corrected and normalised Counts.

5.1 Averaging

Daily averages of the surface solar radiation and the spectrally-resolved solar surface irradiance are calculated from the instantaneous derived surface radiation data following the method published in Diekmann et al., 1988:

Equation 5-1


$$SIS_{DA} = SIS_{CLSDA} \frac{\sum_{i=1}^n SIS_i}{\sum_{i=1}^n SIS_{CLS_i}}$$

SIS_{DA} is the daily average of SIS. SIS_{CLSDA} is the daily averaged clear sky SIS, SIS_i the calculated SIS for satellite image i and SIS_{CLS_i} the corresponding calculated clear sky SIS.

The number of images available during a day is denoted by n .

The larger the number of available images per day, the better the daily cycle of cloud coverage can be resolved, increasing the accuracy of the daily average of SIS. Please note that the diurnal cycle of the solar zenith angle is implicitly accounted for by using the clear sky daily mean SIS value in the averaging.

A minimum number of three available pixels per day is required to derive the daily mean for this specific pixel. The monthly average is calculated from the daily means of this month on pixel basis as arithmetic mean with a required number of 10 existing daily means.

	Algorithm Theoretical Basis Document Meteosat Climate Data Records of Surface Radiation SARAH-2.1	Doc. No: SAF/CM/DWD/ATBD/METEOSAT/HEL Issue: 2.4 Date: 22.01.2019
---	--	--

The conversion from the irregular satellite projection to the regular 0.05 x 0.05 degree regular lon-lat-grid is conducted with the gnu-MAGIC / SPECMAGIC gridding tool based on a nearest-neighbour method.

The temporal averaging of the SDI, i.e, the direct normalized surface solar radiation, DNI, and the direct surface solar radiation, SID, as well as of the SRI are conducted identical as for the surface solar irradiance, SIS, and are not repeated here.

5.2 Sensitivity and dependence on input parameters of SIS / SDI / SRI

The sensitivity of the surface solar radiation on the input parameters is discussed. The section provides the uncertainty or sensitivity of SIS in relation to the input parameters. The error and accuracy of SIS is assessed by comparison with in-situ data and provided in the validation report. Beside the clear sky index, which is derived from satellite observations, aerosol and water vapour have a significant effect on the attenuation of the solar irradiance as well, while the impact of the surface albedo on the downwelling solar radiation is rather weak. A full uncertainty assessment can be found in RD 1, thus only the main results are summarized.

5.2.1 Water vapor:

The sensitivity of the solar surface radiation on the integrated water vapour is higher for low water vapour amounts and low solar zenith angles. The total surface irradiance shows a stronger sensitivity to uncertainties in the integrated water vapour than the direct solar radiation. Overall uncertainties in the integrated water vapour of about 1 to 2 mm translate to uncertainties of approx. 3 W/m², with slightly larger values under low water vapour conditions, and less uncertainty under high water vapour levels.

5.2.2 Ozone


The sensitivity of the solar surface radiation on the integrated ozone amount is in the order of 1 W/m² for typical ozone variation within the SEVIRI disk. Again the sensitivity of the solar irradiance on ozone is slightly higher than that given for the direct irradiance.

5.2.3 Aerosols

The sensitivity of the surface solar radiation to uncertainties in aerosol information is mainly governed by the aerosol optical depth (AOD). While the sensitivity of the direct irradiance by aerosols is completely governed by the AOD, the total surface solar radiation is also sensitive to uncertainties in the aerosol type, expressed by the single scattering albedo and the asymmetry parameter. In all cases, the sensitivity does also depend on the solar zenith angle.

The sensitivity on uncertainties in the AOD is much higher for the direct irradiance than for the global irradiance. Typical uncertainties in the monthly mean aerosol optical depth of 0.1 relative to a background of AOD=0.2 leads to uncertainties in SIS of about 10 W/m² for a solar zenith angle of 60 degree and about 20 W/m² for solar zenith angle of 0 degree, both for cloudless sky (values are approx. three times higher for SID). However, for cloudy conditions these uncertainties are reduced significantly with increasing cloud optical depth.

For the total surface solar radiation, additional uncertainties result from the assumptions on the aerosol optical properties, which can be in the same order of magnitude. Uncertain aerosol information are one of the major sources of the errors in the retrieval of surface solar

	Algorithm Theoretical Basis Document Meteosat Climate Data Records of Surface Radiation SARAH-2.1	Doc. No: SAF/CM/DWD/ATBD/METEOSAT/HEL Issue: 2.4 Date: 22.01.2019
---	--	--

radiation from satellite on short time scales. On the daily and monthly time scales, however, the aerosol impacts are substantially reduced compared to the instantaneous values. Further details are given in RD 1.

5.2.4 Surface albedo

The sensitivity of clear sky SIS on uncertainties and errors in the surface albedo is comparably small. Deviations of +/- 0.1 in the surface albedo lead to deviations in clear sky SIS of +/- 1%. The effect is almost linear. Errors in the surface albedo are expected to be typically less than 0.1, with exception of snow covered surfaces, where higher errors might occur. The effect is pre-dominantly independent on the clear sky atmospheric state.

5.2.5 Clear sky index


The clear sky index is calculated from the effective cloud albedo using Equation 3-10. For $CAL > 0.8$ the clouds are optically rather thick and the uncertainty in the solar irradiance is small in absolute terms. Therefore, it is focused on the region between 0 and 0.8. Here any uncertainty in the effective cloud albedo leads to identical uncertainty in the clear sky index. As only the uncertainty arising from the cloud index is of interest and a negligible contribution of the clear sky irradiance to the overall uncertainty can be assumed.

As a result of the definition of the clear sky index an uncertainty of x% translates directly in the identical relative uncertainty for the solar irradiance, meaning a 3 % uncertainty in the effective cloud albedo leads to a 3 % uncertainty in the solar irradiance.

For the direct surface solar radiation, the sensitivity on the clear sky index is larger. An uncertainty of 2% for the clear sky index results in an uncertainty of about 10 % in the direct irradiance, demonstrating the importance of an accurate clear sky index on the direct irradiance. Further information can be found in RD 1.

5.3 Assumption, limitations and future improvements

- The high clear sky reflection over bright surfaces (e.g., desert regions) reduces the contrast between clear sky reflection and cloudy-sky reflection. This leads to higher uncertainties in CAL and errors in the calculation of SIS and SDI over bright surfaces. The modified approach for the clear sky reflection improves the accuracy of SIS over bright surfaces, but the accuracy is still significantly lower than for other surfaces.
- In regions with long-lasting cloud cover the modified approach for the clear sky reflection overestimates the clear sky reflection. This results in an underestimation of the effective cloud albedo and an overestimation of the solar surface radiation.
- The accuracy of aerosol information is unknown in several regions of the world due to missing ground measurements. Any uncertainty in the aerosol information affects the accuracy of the surface solar radiation (in particular for the direct solar radiation), especially in regions that are dominated by cloudless sky.
- The use of a monthly climatology for the aerosol optical depth reduces the ability to correctly describe the effects of changes in the aerosol concentration on the clear-sky surface solar radiation. For future improvements, available sources of temporally-varying aerosol information will be assessed to be included in the retrieval of the surface radiation.
- The quality of the direct irradiance strongly depends on the quality of the information about the atmospheric state, especially the aerosol information, the integrated water vapour and the clear sky index.

	<p align="center">Algorithm Theoretical Basis Document Meteosat Climate Data Records of Surface Radiation SARAH-2.1</p>	<p>Doc. No: SAF/CM/DWD/ATBD/METEOSAT/HEL Issue: 2.4 Date: 22.01.2019</p>
---	--	--

- The gnu-MAGIC / SPECMAGIC clear sky model does currently not consider topography for the clear sky surface radiation calculations. The integrated water vapour content is adjusted to account for its reduction at higher elevations; the impact of elevation on aerosol optical depth is considered on the coarse grid resolution. Only the effect of modified Rayleigh scattering is not accounted for, which is considered to be small.

6 Sunshine Duration

Basis for the retrieval of satellite-based sunshine duration (SDU) are the SARAH-2 DNI data and the WMO threshold for bright sunshine, which is defined by $DNI \geq 120 \text{ W/m}^2$. SDU is derived by the ratio of sunny slots to all slots during daylight:

Equation 6-1

$$SDU = \text{daylength} \times \frac{\sum_{i=1}^{\text{iday}} (W_i(\text{sunny slot}_i))}{\# \text{daylight slots}}$$

The daylength is calculated depending on the date, longitude and latitude. The daylength is restricted by a threshold of the solar elevation angle (SEA) of 2.5° (Kothe et al., 2013). The W_i indicates a weighting of sunny slots depending on the number of surrounding cloudy and sunny grid points, which is discussed in more detail in section 5.1. The number of daylight slots ($\# \text{ daylight slots}$) describes the maximum number of Meteosat observations (slots) per grid point and per day during daylight. Daylight is defined by the time where the SEA exceeds 2.5° .

6.1 Weighting of sunny slots

A sunny slot corresponds to a DNI value of 120 W/m^2 or larger. SARAH-2.1 provides instantaneous DNI data every 30 minutes. Therefore, without weighting, in Equation 6-1 one sunny slot would correspond to a 30 minutes time window. In reality this is only the case in bright weather situations. If there are clouds in the surrounding area of a grid point, there is a probability that not the whole 30 minutes are sunny. This is also valid in the opposite case, when a cloudy grid point has sunny grid points in its near surrounding's. This fact should be accounted for in the retrieval of SDU by using the information of the 24 surrounding grid points (see Figure 5-1).

In addition the information of two successive time steps is incorporated.

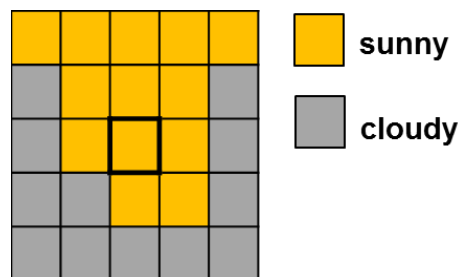


Figure 5-1: Demonstration for accounting for surrounding grid points. The target grid point is marked in the centre.

In a first step for each grid point the number of sunny grid points in an environment of 24 grid points is summed up. This is done for each daytime slot. The number of each time step is combined with the number of the previous time step to incorporate also the temporal movement of clouds in a simplified way (see Equation 6-2).

Equation 6-2

$$N_1 = \# \text{sunny area}_1 \times 0.04$$

$$N_i = (\# \text{sunny area}_i + \# \text{sunny area}_{i-1}) \times 0.02$$

The resulting number N is 1 in case that all grid points are sunny, and 0 in the case that no grid point is sunny.

In a second step the impact of cloudy and sunny grid points on the temporal length of one time slot is estimated. The grid points Sgp get the value 1 in case that $DNI \geq 120 \text{ W/m}^2$ and 0 in case $DNI \leq 120 \text{ W/m}^2$. The opposite is done for Cgp , where the grid point gets the value 1 in case that $DNI \leq 120 \text{ W/m}^2$ and 0 in case $DNI \geq 120 \text{ W/m}^2$. Two constant values were empirically determined to correct the influence of sunny or cloudy grid points.

Equation 6-3 $Sgp_i = Sgp_i \times N_i$ with lower limit of N_i is set to $C1$
Equation 6-4 $Cgp_i = Cgp_i \times (N_i \times C2)$

The sum of Sgp and Cgp is the fraction of the time, which one slot contributes to the sunshine duration of a slot.


Equation 6-5 $W_i(\text{sunny slot}_i) = Sgp_i + Cgp_i$

The final sunshine duration in hours is derived by Equation 6-1.

6.2 Assumption, limitations and future improvements

The constants $C1$ and $C2$ are empirical estimations, which were derived by simple test calculations using about 250 reference stations in Germany only. These tests have to be more systematic and for a larger and more representative number of reference stations. Another possible improvement can be done for the impact of the surrounding grid points. This influence is only estimated, as the real cloud motion is unknown by the retrieval algorithm. Using auxiliary input fields, such as cloud motion vectors, could further improve the sunshine duration.

A limitation of the final data record are shaped artefacts, which are most obvious in cloud free areas, such as deserts. These artefacts are a result of the combination of 30 minutes instantaneous data, where the threshold of $DNI \geq 120 \text{ W/m}^2$ is already reached at the border of the Meteosat disk.

	Algorithm Theoretical Basis Document Meteosat Climate Data Records of Surface Radiation SARAH-2.1	Doc. No: SAF/CM/DWD/ATBD/METEOSAT/HEL Issue: 2.4 Date: 22.01.2019
---	--	--

7 Improvements relative to the released previous versions of the CM SAF Surface Radiation data records.

7.1 Improvements compared to the MVIRI Surface Radiation data record

The length of the data record has substantially been extended compared to the CM SAF MVIRI CDR.

Special care has been taken in order to improve the homogeneity of the CDR. The available CM SAF MVIRI CDR exhibits some breaks and inhomogeneities in Europe before 1994 (Sanchez-Lorenzo et al., 2013). There are also indications of artificial shifts in the data record in other regions (Brinckmann et al., 2013). Corrupted raw data are, at least partly, the source of these breaks and inhomogeneities. Due to problems with data transmission only every second line of the broadband visible channel had been transmitted during night and twilight hours. This has been considered within the processing of the first CM SAF MVIRI only data record (RD.1), according to the EUMETSAT documentation. However, much more hours and time periods are affected. For these times the lines have been incorrectly interpreted as defined due to a missing no-data value in the raw images. Moreover, many other images are corrupted without being documented or listed as such. The CM SAF team performed a visual inspection of the images in order to detect all corrupted or incomplete images. This visual inspection is very time consuming, but the only possibility to avoid the use of corrupted or incomplete images. Some flaws as missing or black lines can be treated by interpolation (see section 3.5) or by assigning non-defined values. However, many corrupted images cannot be used and have to be disregarded within the reprocessing in order to avoid corruption of the retrieved solar surface irradiance.

The transition between MFG and MSG is a source for serious breaks and inhomogeneities due to the change in the spectral observations from the MVIRI to the SEVIRI instruments. Respective issues have been investigated and resolved (Posselt et al. 2011; 2013). For the generation of the current SARAH data record an artificial visible broadband channel has been used.

The IDL interpolation routine leads to circle structures in the images and has been replaced by an algorithm of R. Müller, developed within gnu-MAGIC.


A bug in the routine for the calculation of the pixel scanning time has been fixed.

7.2 Improvements compared to the first version of SARAH data record (MVIRI/SEVIRI Ed.2)

The spectral-resolved surface solar radiation (SRI) and the sunshine duration (SDU) is provided as part of SARAH-V2 and its extension SARAH V2.1.


The length of the data record will be extended compared to the available CM SAF SARAH CDR.

Additional, special care has been taken in order to further improve the homogeneity of the CDR. In particular the SARAH V1 CDR has a tendency to provide lower values after 2006, indicating a possible inhomogeneity in the transition from the MVIRI to the SEVIRI instruments. The homogeneity of the MVIRI – SEVIRI transition has been improved compared to the SARAH V1 CDR.

	<p align="center">Algorithm Theoretical Basis Document Meteosat Climate Data Records of Surface Radiation SARAH-2.1</p>	<p>Doc. No: SAF/CM/DWD/ATBD/METEOSAT/HEL Issue: 2.4 Date: 22.01.2019</p>
---	--	--

The geometric viewing angle effect on the cloud albedo has been considered using an empirical formula depending on the satellite zenith angle.

The integrated water vapour from ERA-Interim has been adjusted to include an elevation dependency. This does result in more realistic clear-sky surface radiation calculations, and, subsequently, has the largest impact on SIS and DNI in regions with high clear-sky contributions.

	Algorithm Theoretical Basis Document Meteosat Climate Data Records of Surface Radiation SARAH-2.1	Doc. No: SAF/CM/DWD/ATBD/METEOSAT/HEL Issue: 2.4 Date: 22.01.2019
---	--	--

8 References

Bellouin, N., Quaas, J., Morcrette, and J.-J., Boucher, O., 2013: Estimates of aerosol radiative forcing from the MACC re-analysis, *Atmos. Chem. Phys.*, **13**, 2045-2062.

Benedetti, A., Morcrette, J.-J., Boucher, O., Dethof, A., Engelen, R.J., Fisher, M., Flentje, H., Huneeus, N., Jones, L., Kaiser, J.W., Kinne, S., Mangold, A., Razinger, M., Simmons, A.J., Suttie, M., Aerosol analysis and forecast in the European Centre for Medium-Range Weather Forecasts Integrated Forecast System: 2. Data assimilation, *J. Geophys. Res.*, 2009, 114, D13205

Bento, V., 2016: Improving Land Surface Temperature retrievals over mountainous regions, Poster presented at the DUE GlobTemperature User Consultation Meeting #4, Lisbon, June 2016.

Beyer H. G., Costanzo C. and Heinemann, D., 1996: Modifications of the Heliosat procedure for irradiance estimates from satellite images, *Solar Energy*, **56**, 207-212.

Brinckmann S, Trentmann J, Ahrens B. Homogeneity Analysis of the CM SAF Surface Solar Irradiance Dataset Derived from Geostationary Satellite Observations. *Remote Sensing*. 2014; 6(1):352-378.

Cano D., Monget J. M., Albuissou M., Guillard H., Regas N., and Wald, L. A method for the determination of the global solar-radiation from meteorological satellite data, *Solar Energy*, 1986, 37, 31-39.

Cros, S.; Albuissou, M.; Wald, L., Simulating Meteosat-7 broadband radiances using two visible channels of Meteosat-8. *Solar Energy*, 2006, 80, 361–367.

Dagestad, K.-F. Mean bias deviation of the Heliosat algorithm for varying cloud properties and sun-ground-satellite geometry, *Theor. Appl. Climatol.*, 2004, 79, 215–224, DOI 10.1007/s00704-004-0072-5

Dee, D., et al., The ERA-Interim reanalysis: configuration and performance of the data assimilation system, *Q. J. R. Meteorol. Soc.*, 2011, 137: 553–597,


Diekmann, F.J., S. Happ, M. Rieland, W. Benesch, G. Czeplak, F. Kasten, An operational estimate of global solar irradiance at ground level from METEOSAT data: results from 1985 to 1987, 1988, *Meteorol. Rdsch.*, 41, 65-79.

Dürr B., and Zelenka A. Deriving surface global irradiance over the alpine region from Meteosat second generation data by supplementing the Heliosat method, *International Journal of Remote Sensing*, 2009, 5821-5841, DOI 10.1080/01431160902744829.

Hammer A., Heinemann D., Hoyer C., Kuhlmann R., Lorenz E., Müller R., and Beyer H. G. Solar energy assessment using remote sensing technologies, *Remote Sens. Environ.*, 2003, 86, 423--432.

Hammer, A., 2000. Anwendungsspezifische Solarstrahlungsinformationen aus Meteosat-Daten. Phd, School of Mathematics and Natural Sciences, University of Oldenburg.

Hess, M.; P. Köpke; I. Schult: Optical Properties of Aerosols and Clouds: The Software Package OPAC. *Bull. Amer. Meteor. Soc.*, 1998, 79, 831-844.

	Algorithm Theoretical Basis Document Meteosat Climate Data Records of Surface Radiation SARAH-2.1	Doc. No: SAF/CM/DWD/ATBD/METEOSAT/HEL Issue: 2.4 Date: 22.01.2019
---	--	--

Kinne, S., Schulz M., Textor C. et al. : An AeroCom initial assessment – optical properties in aerosol component modules of global models, *Atmos. Chem. Phys.*, 2006, 6, 1815-1834.

Köpke P.; Hess M.; Schult I.; Shettle E., Global aerosol data set. *Tech. Rep.*, 1887, 243, MPI Meteorology, Hamburg.

Kothe, S., Good, E. Obregón, A. Ahrens, B., Nitsche, H.: Satellite-Based Sunshine Duration for Europe. *Remote Sens.* 2013, 5(6), 2943-2972; doi:10.3390/rs5062943

Mayer B.; A. Kylling, Technical note: “The libRadtran software package for radiative transfer calculations - description and examples of use.” *Atmos. Chem. Phys.*, 2005, 5, 1855-1877.

Morcrette, J. J., Boucher, O., Jones, L., Salmond, D., Bechtold, P., Beljaars, A., Benedetti, A., Bonet, A., Kaiser, J. W., Razinger, M., Schulz, M., Serrar, S., Simmons, A. J., Sofiev, M., Suttie, M., Tompkins, A. M., Untch, A., Aerosol analysis and forecast in the European Centre for Medium-Range Weather Forecasts Integrated Forecast System: Forward modelling, *J. Geophys. Res.*, 2009, 114

Müller, R.W. et al., Report of the HELIOSAT-3 software package for solar irradiance retrieval, all sky working version” *EU report of the Heliosat-3 project (www.heliosat3.de), NNE5-2000-00413*, 2003

Mueller, R., U. Pfeifroth, and C. Traeger-Chatterjee, 2015a: Towards Optimal Aerosol Information for the Retrieval of Solar Surface Radiation Using Heliosat. *Atmosphere*, 6, 863-878.

Mueller, R.W., K.F. Dagestad, P. Ineichen, M. Schroedter-Homscheidt, S. Cros, D. Dumortier, R., Kuhlemann R. ; Olseth J.A.; Piernavieja G.; Reise C.; Wald L.; Heinemann D.; Rethinking satellite based solar irradiance modelling – The SOLIS clear sky module”, *Rem. Sens. Envir.*, 2004, 91, 160-174.

Mueller, R.W., Matsoukas, C. Behr, H.D., Gratzki, A. Hollmann, R., MAGIC - The CM-SAF operational scheme for the satellite based retrieval of solar surface irradiance - a LUT based eigenvector hybrid approach. *Remote Sensing of Environment*, 2009, 113, 1012-1024.


Mueller, R.; Behrendt, T.; Hammer, A.; Kemper, A. A New Algorithm for the Satellite-Based Retrieval of Solar Surface Irradiance in Spectral Bands. *Remote Sens.* 2012, 4, 622-647.

Mueller, R., and C. Träger-Chatterjee, 2014: Brief Accuracy Assessment of Aerosol Climatologies for the Retrieval of Solar Surface Radiation. *Atmosphere*, 5, 959-972.

Müller, R., U. Pfeifroth, C. Träger-Chatterjee, J. Trentmann, and R. Cremer, 2015b: Digging the METEOSAT Treasure—3 Decades of Solar Surface Radiation. *Remote Sensing*, 7, 8067-8101.

Perez, R., Seals, R., Zelenka, A., Production of Site/Time-specific Hourly Irradiances - Satellite Remote Sensing vs. Network Interpolation, in Production of Site/Time-specific Irradiances from Satellite and Ground Data, *published by New York State Energy Research and Development Authority* , 1998, Report 98-3.

Perez, R. et al., 2001, Solar resource assessment: A review, in Solar Energy - The state of the art, published by James & James Science Publishers, 497-562.

	Algorithm Theoretical Basis Document Meteosat Climate Data Records of Surface Radiation SARAH-2.1	Doc. No: SAF/CM/DWD/ATBD/METEOSAT/HEL Issue: 2.4 Date: 22.01.2019
---	--	--

Posselt R, Mueller R, Stöckli R, Trentmann J. Spatial and Temporal Homogeneity of Solar Surface Irradiance across Satellite Generations. *Remote Sensing*. 2011; 3(5):1029-1046.

Posselt R., Müller, R.W., Stöckli R., Trentmann, J., 2012, Remote sensing of solar surface radiation for climate monitoring - the CM-SAF retrieval in international comparison, *Remote Sens. Environ.*, 118, 186-198, doi: 10.1016/j.rse.2011.11.

Posselt, R., Mueller R., Trentmann J., Stoeckli R., Liniger M., Extension of the CM SAF surface radiation climatology (MAGIC SOL) beyond Meteosat First Generation Satellites, accepted for publication in *Remote Sensing of Environment*, 2013.

Rigollier C., Lefevre M., Blanc P., and Wald L.: The operational calibration of images taken in the visible channel of the meteosat series of satellites, *J. Atmos. Ocean. Technol.*, 2002, 19, 1285-1293.

Rigollier C., Lefevre M., and Wald L., 2004: The method Heliosat-2 for deriving shortwave solar radiation from satellite images, *Solar Energy*, 77, 159–169.

Sanchez-Lorenzo, A., Wild, A.M., Trentmann, J., 2013. Validation and stability assessment of the monthly mean CM SAF surface solar radiation dataset over Europe against a homogenized surface dataset (1983–2005), *Remote Sens. Environ.*, 134, 355-366, doi: 10.1016/j.rse.2011.11. doi: 10.1016/j.rse.2013.03.012

Skartveit A., Olseth J., Tuft M., 1998: An hourly diffuse fraction model with correction for variability and surface albedo. *Solar Energy*, 63, 173–183.

Wald, L..et al., SoDa: A project for the integration and exploitation of networked solar radiation databases, in *Environmental Communication in the Information Society, Published by the International Society for Environmental Protection*, Vienna, Austria, Editors: Pillmann and Tochtermann, 2002, 713-720.

Zelenka, A., R. Perez, R. Seals, D. Renne, 1999: Effective Accuracy of Satellite-Derived Hourly Irradiances, *Theor. Appl. Climatol.*, 62, 199 – 207.

9 Glossary – List of Acronyms

AOD	Aerosol Optical Depth
CAL	Effective Cloud Albedo
CDOP	Continuous Development and Operational Phase
CDR	Climate Data Record
CM SAF	Satellite Application Facility on Climate Monitoring
DWD	Deutscher Wetterdienst
DNI	Direct Normal Irradiance
ECMWF	European Centre for Medium-Range Weather Forecast
ECV	Essential Climate Variable
ERA	ECMWF Reanalysis
GADS/OPAC	Global Aerosol Data Set / Optical Properties of Aerosols and Clouds
GCOS	Global Climate Observing System
GERB	Geostationary Earth Radiation Experiment
K	Clear sky index
LUT	RTM based Look-Up-Table
MAD	Mean of absolute deviation over several days or months
MVIRI	Meteosat Visible-InfraRed Imager
MACC	Monitoring Atmospheric Composition and Climate
RTM	Radiative Transfer Model
SARAH	Surface Solar Radiation Data records – Heliosat
SDI	Surface Direct Irradiance (consist of SID and DNI)
SDU	Sunshine Duration
SEA	Sun Elevation Angle
SEVIRI	Spinning Enhanced Visible and InfraRed Imager
SID	Surface Incoming Direct radiation, commonly called direct irradiance
SIS	Surface Incoming Solar radiation, commonly called global irradiance or surface solar irradiance

SRI	Spectral Resolved Irradiance
SSA	Single Scattering Albedo
SZA	Solar Zenith Angle